

LABORATORY STUDIES OF MERCURY ANALOGUE MATERIALS: OPTICAL SPECTROSCOPY AND SPACE WEATHERING SIMULATION EXPERIMENTS. L. V. Moroz^{1,2}, A. Maturilli², J. Helbert², S. Sasaki³, A. Bischoff¹, ¹Institut für Planetologie, Universität Münster, Wilhelm-Klemm Str. 10, 48149 Münster, Germany, ²DLR-Institut für Planetenforschung, Rutherfordstr. 2, 12489 Berlin, Germany; Ljuba.Moroz@dlr.de; ³Nat. Astron. Observatory of Japan, Mizugawa, Oshu, Japan.

Introduction: MERTIS (Mercury Thermal Infrared Imaging Spectrometer) is a part of ESA's BepiColombo mission payload [1] and will map Mercury's surface from 7 to 14 μm with high spatial resolution.

To support MERTIS and for cross-calibration with other instruments onboard BepiColombo (SYMBIO-SYS) and MESSENGER (MASCS) a list of Mercury analogue materials has been compiled [2].

Here we report the results of spectral reflectance measurements of these analogues from 0.5 to 18 μm . We compare the TIR reflectance spectra of the samples to their emissivity spectra (data from Berlin Emissivity Database [3]) to evaluate deviations from Kirchhoff's law for biconical reflectance.

In addition, we report on a space weathering simulation experiment on plagioclase and discuss future space weathering simulation experiments relevant to Mercury and other solar system bodies with FeO-poor surfaces.

Samples and Experimental Procedures: The selected Mercury analogue materials [1] include: plagioclases (albite, oligoclase, andesine-labradorite, anorthite), orthoclase, enstatite, diopside, forsterite, elemental S and the Apollo 16 lunar highland soil 62231. For the spectral studies we prepared size fractions of <25, 25-63, 63-125, and 125-250 μm (except for the lunar soil). Separates >25 μm were wet-sieved.

The samples were characterized in terms of chemical composition, mineralogy, and grain size distribution.

Biconical reflectance spectra were acquired from 0.5 to 18 μm at the DLR Institute of Planetary Research using a Bruker IFS88 FTIR-spectrometer equipped with a "Seagull™" reflectance accessory.

To simulate micrometeorite bombardment on an FeO-poor target appropriate to Mercury, pressed pellets of powdered andesine were irradiated with a nanosecond pulsed laser at the National

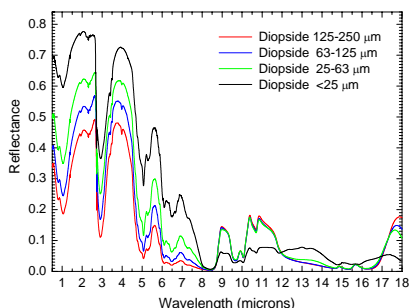


Fig. 1. Biconical reflectance spectra of diopside separates between 0.5 and 18 μm .

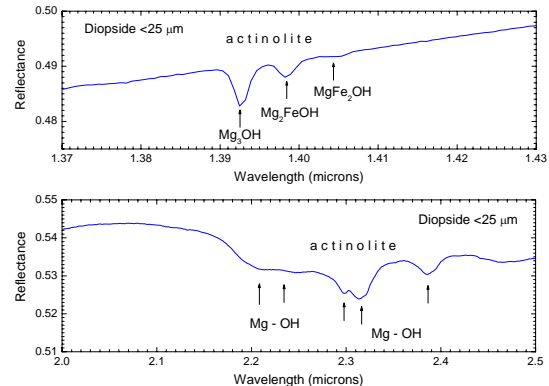


Fig. 2. Identification of weak actinolite absorption bands (Metal-OH overtones) in NIR reflectance spectra of a diopside powder.

Astronomical Observatory of Japan (see [4] for details); their reflectance spectra were measured with the above equipment.

Results: Examples of biconical reflectance spectra are shown in Fig. 1 for diopside separates. Note the significant variations in reflectance values and absorption band contrasts with grain size. Detailed analysis of weak absorption features in high-resolution NIR reflectance spectra enabled the identification of OH and/or H₂O-bearing weathering products in the samples (see, e.g., Fig 2).

Kirchhoff's law ($E=1-R$) is valid within certain limits for directional-hemispherical reflectance [5], while most reflectance data on minerals and rocks are acquired at biconical geometry. Thus, it is important to test the validity of Kirchhoff's law for biconical reflectance for various samples – slabs, particulates of various particle sizes, loose and packed fine powders. We had the unique opportunity to measure identical samples using the same instrument (Bruker IFS88) operating at emissivity (E) and biconical reflectance (R_b) modes. The procedures for spectral emission measurements are described in detail in [6].

We compared the E with the $1-R_b$ values in the TIR for Mercury analogues and quartz separates. For loose powders at ambient pressures $1-R_b$ deviation from E does not exceed 3%, despite significantly different viewing geometries of E and R_b measurements (Fig. 3a,b). We found no systematic differences in band shapes and relative band contrasts. However, transparency features that are absent in biconical reflectance spectra of coarse-grained samples (63-125, 125-250 μm), are evident in the corresponding emission spectra (e.g., Fig. 3b). Deviations of $1-R_b$ from E are very significant in the cases of slabs (Fig. 3c) and compact fine powders (Fig. 3d). Packing effects are much less pronounced

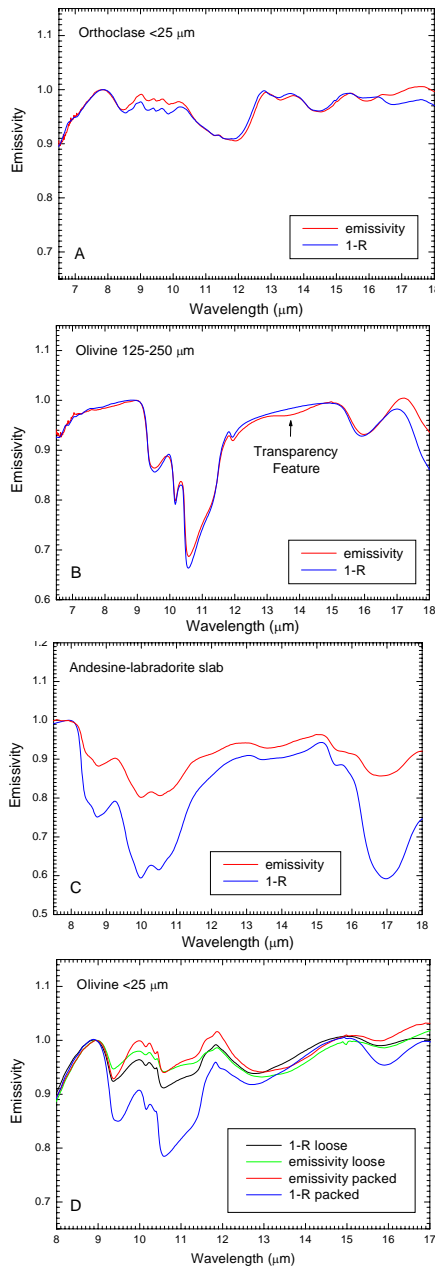


Fig. 3. TIR E vs. $1-R_b$ for: loose powders of (A) orthoclase ($<25\text{ }\mu\text{m}$) and (B) olivine Fo_{90} ($125\text{-}250\text{ }\mu\text{m}$), (C) andesine-labradorite unpolished slab, and (D) loose and packed fine ($<25\text{ }\mu\text{m}$) olivine powders

in emission (at least at ambient pressures) than in biconical reflectance. These effects have to be taken into account when comparing remote sensing emission spectra of planetary surface areas covered with bare rocks or compact crusts with lab spectra acquired at biconical geometry on slabs or simulated crusts.

Thus, for quantitative analyses of such surfaces laboratory emission measurements are mandatory, although they are also preferable in cases of particulate surfaces. Note that our results were performed at ambient pressures and may not be applicable in low pressure environments.

Fig. 4 shows reflectance spectra of two andesine-labradorite ($\text{An}_{47.5}$) pellets, non-irradiated and irradiated once ($20\text{ mJ } \times 1$) or twice ($20\text{ mJ } \times 2$) with a nanosecond pulsed laser to simulate micrometeorite bombardment on a very FeO-poor (0.77 wt.% FeO) target. No darkening is evident even after the highest irradiation dose. A mild NIR reddening and decrease in the TIR spectral contrast are observed. The latter effects are probably due to surface roughness changes produced by the laser, though further analysis is needed for confirmation. Our result – weak reddening and no darkening – differs from those of previous nanosecond pulse laser irradiation experiments [e.g., 4] and indicates that the presence of FeO in the target minerals is crucial to produce space darkening and reddening of planetary regoliths, induced by micrometeorite bombardment.

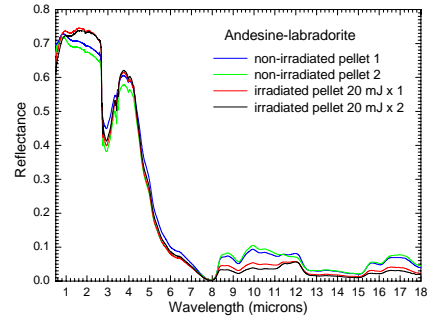


Fig. 4. Biconical reflectance spectra ($0.5\text{-}18\text{ }\mu\text{m}$) of non-irradiated and laser-irradiated plagioclase pellets.

We plan new space-weathering simulation experiments (e.g., irradiation of Fe-free and Fe-poor targets with low-energy ions) to find out how such materials would respond to irradiation with solar wind plasma in space. The results of such experiments should provide crucial information not only on space weathering effects on Mercury, but also regarding space weathering on certain asteroids, such as, for example, a ROSETTA target 2867 Steins.

Acknowledgments: We thank I. Büttner, K. Schmale, T. Grund, M. Ahmed, U. Heitmann, T. Jording, K., Prof. H. Palme, Dr. R. Wäsch for assistance in sample preparation and analyses. This work was supported by DLR MERTIS project 50 QW 0502.

References: [1] Benkhoff J. et al. (2006) *Adv. Space. Res.*, 38, 647-658. [2] Helbert J. et al., *Adv. Space. Res.*, 40, 272-279. [3] Maturilli A. et al., *Planet & Space Sci.*, 54, 1057-1064. [4] Yamada M. et al. (1999) *Earth Planets Space*, 51, 1255-1265. [5] Salisbury J. W. et al. (1994) *J. Geophys. Res.*, 99, 11897-11911. [6] Maturilli A. et al. (2006) *Planet & Space Sci.*, 54, 1057-1064.